



1 A calculation method of unsaturated soil water content based on 2 thermodynamic equilibrium

3 Danhui Su¹, Jianwei Zhou^{1,2}, Zuocong Yin³, Haibo Feng¹, Xiaoming Zheng¹, Xu Han¹, Qingqiu Hou¹

4 ¹School of Environmental Studies, China University of Geosciences, Wuhan, 430085, China

5 ²Key Laboratory of Mine Ecological Effects and Systematic Restoration, Beijing, 100081, China

6 ³Centralsouth Bureau of China Metallurgical Geology Bureau, Wuhan, 430080, China

7 *Correspondence to:* Jianwei Zhou (jw.zhou@cug.edu.cn)

8 **Abstract.** Accurate determination of soil water content is crucial for studying the local ecological water cycle, agriculture,
9 forests and grasslands management, slope stability, environmental processes, and ecological problems. Current measurement
10 methods of soil water content have challenges with the complicated operation, high costs, significant system errors, and soil
11 type-specific accuracy. In this study, we proposed an alternative method to measure soil water content using the ratios of mass
12 and density of water to vapor based on system science and thermodynamics. We derived the mass ratio and density ratio of
13 water to vapor as a function of temperature from published data and validated the accuracy of the proposed method using
14 observed temperature, relative humidity, and volumetric water content in two soil textures of medium and fine sand. We further
15 demonstrated that the mass ratio function is independent of the nature of the water-containing media using theoretical and
16 statistical analysis. The absolute error of soil water content between the calculated and measured ones is less than 1% and is
17 positively correlated with temperature. This study significantly improves the measurement accuracy of soil water content,
18 eliminates the effect of water-containing medium on soil water content measuring, and has excellent potential for application
19 in the field soil and even rock water content measurement.

20 1 Introduction

21 Soil is crucial to life on Earth (Weil and Brady, 2017b), and soil water is one of the most critical factors. Determination of soil
22 water content is fundamental in studying soil's physical, chemical, and ecological processes. Soil water is an essential
23 component of the ecological water cycle, as it regulates rainfall infiltration, surface runoff, and evaporation, as well as affecting
24 river flow and local climate (Anh et al., 2015; Daly and Porporato, 2005; Good et al., 2015; Norton et al., 2022). Soil water
25 content plays an essential role in plant growth. It influences the germination and emergence of plant seeds (Nielsen et al.,
26 1995), as well as the health and quality of plants (Ma and Fan, 2020; Satoh and Kakiuchi, 2021), and has a direct impact on
27 forest and agricultural productivity (Breda et al., 2006). Soil water is the primary factor influencing microbial community
28 structure and enzyme activities (Brockett et al., 2012; Ni et al., 2022). On the one hand, it is the basis for microbial survival.
29 On the other hand, soil water content determines the air content and gas diffusion in the soil, thus affecting microbial activity
30 (Hillel, 2008a). The mechanical properties of soil, such as consistency, plasticity, shear strength, etc., depend on soil water



31 content (Hillel, 2008a; Lekshmi et al., 2014). Therefore, it significantly impacts geotechnical engineering structure and slope
32 stability (Ng Charles and Pang, 2000; Rahimi et al., 2010; Xu and Yang, 2018). In general, accurate determination of soil
33 water content is important in geology, hydrology, ecology, agronomy, engineering, and other fields (Ma et al., 2016).
34 Researchers have worked extensively on determining soil water content and have accomplished many critical results.
35 Nevertheless, there are some limitations. Measurement methods of soil water content are often classified as direct and indirect
36 (Shukla, 2013; Topp et al., 2007). The direct method is the thermo-gravimetric method, particularly the oven drying method.
37 The soil sample is dried in an oven at a constant temperature of about 105°C until the weight of the dry soil becomes constant,
38 and the difference in soil weight before and after drying is the soil water content (Pansu and Gautheyrou, 2006; Topp and Ferré,
39 2002). The method is commonly used to determine soil water content and is considered a standard. However, the sampling
40 and transportation process may cause disturbance of the soil structure and loss of moisture. Moreover, part of the water is not
41 entirely dried (Wang et al., 2011), and some organic matter may oxidize and decompose at 105°C (Hillel, 1980; Lekshmi et
42 al., 2014). Therefore, the method may produce a significant systematic error.

43 Indirect methods measure the soil's physical or chemical property that depends on its water content. They include the radiation
44 methods (neutron probe, gamma-ray attenuation, nuclear magnetic resonance) (Klenke and Flint, 1991; Manalo et al., 2003;
45 Strati et al., 2018), dielectric methods (time-domain reflectometry, frequency domain reflectometry, amplitude domain
46 reflectometry, capacitive technique) (Moroizumi and Sasaki, 2008; Noborio, 2001; Sheets and Hendrickx, 1995; Whalley et
47 al., 1992; Xu et al., 2012), remote sensing methods (microwave remote sensing and ground-penetrating radar) (Huisman et al.,
48 2003; Jackson, 2002; Liu et al., 2019; Njoku and Entekhabi, 1996), and optical methods (fiber optic sensor technique and near-
49 infrared optical technique) (Alessi and Prunty, 1986; Lekshmi et al., 2014; Lim et al., 2020; Robinson et al., 2008). Radiation
50 methods measure soil water content by the property of radioactive substances concerning soil moisture. Although accurate and
51 rapid, they are costly to use and have risks of radiation exposure (Jarvis and Leeds-Harrison, 1987). The dielectric methods
52 measure soil water content utilizing the dielectric properties determined by soil moisture. They are quick and repeatable, but
53 they ignore the impact of temperature on the soil's dielectric properties and have a considerable measurement error (Noborio,
54 2001). Remote sensing methods use electromagnetic energy emitted or reflected from the land surface. They can obtain the
55 soil water content over a large area, while they have a shallow measurement depth and low measurement accuracy. In addition,
56 the results could be influenced by the nature of the soil and vegetation cover (Bogena et al., 2015). Optical methods capitalize
57 on changes in the characteristics of the incident and reflected light passing through the soil to determine the soil water content.
58 The methods allow distributed remote measurements and are resistant to interference, but they are expensive, and the soil type
59 and surface roughness significantly impact measurement accuracy (Robinson et al., 2008). In summary, current measurement
60 methods of soil water content have challenges with the complicated operation, high costs, significant system errors, and soil
61 type-specific accuracy.

62 To address the issues mentioned above, we propose a new determination and calculation method for soil water content based
63 on system science and thermodynamics, which minimizes the impact of soil type and improves measurement accuracy. This
64 study presents the relationship between soil water content and the mass ratio and density ratio of water to vapor at



65 thermodynamic equilibrium. Sandbox experiments construct the mass ratio of water to vapor as a function of temperature.
66 Furthermore, the mass ratio function is independent of the nature of the water-containing media, according to theoretical
67 analysis and statistical results. The absolute error of soil water content between the calculated and measured is less than 1%
68 and is positively correlated with temperature.

69 **2 Theory and calculation**

70 **2.1 Theory**

71 **2.1.1 Thermodynamic equilibrium**

72 Unsaturated soils consist of mineral particles and pores which contain water and air, with vapor water being a trace but
73 important component of the air. The total internal energy, volume, and amount of substance of the system are constant,
74 assuming that the water and vapor are in an isolated unary two-phase system and the surface of the mineral particles is the
75 boundary. According to the second law of thermodynamics and the fundamental equations of thermodynamics for open
76 systems (Cui, 2009), when the system is in thermodynamic equilibrium, it satisfies three conditions, which are defined as
77 thermal equilibrium, mechanical equilibrium, and phase equilibrium conditions, and they are necessary and sufficient
78 conditions for the thermodynamic equilibrium of the system (Ansermet and Brechet, 2019).

79 Therefore, when a system is in thermodynamic equilibrium, it is in thermal equilibrium, mechanical equilibrium, and phase
80 equilibrium, which indicates that the internal temperature, pressure, and chemical potential are the same everywhere. There is
81 no heat transfer, water movement (Dexter et al., 2012), and phase transition (Braudeau and Mohtar, 2021). Both the water and
82 vapor contents are constant at this moment.

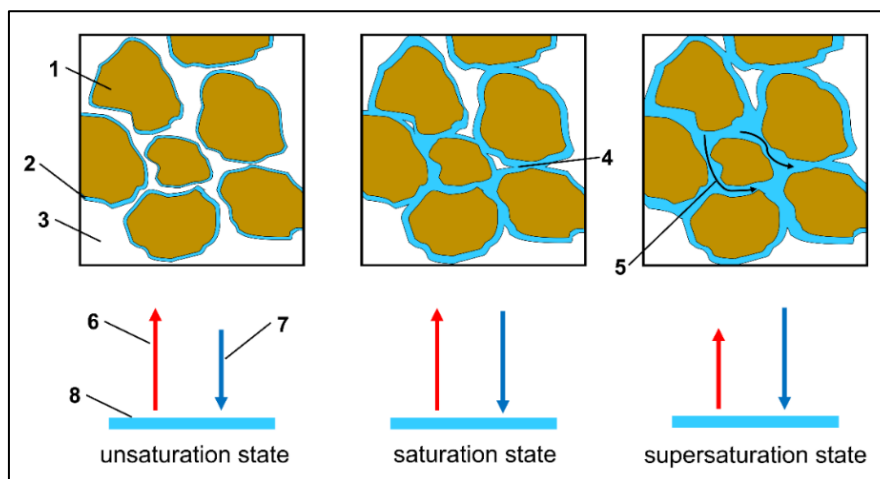
83 **2.1.2 Water equilibrium and transformation in unsaturated soils**

84 Water in unsaturated soils exists mainly in the form of bound and capillary water. The surface of mineral particles can adsorb
85 the surrounding water molecules and generate bound water due to van der Waals and electrostatic interactions between mineral
86 particles and water (Lu and Zhang, 2019; Whalley et al., 2013). Meanwhile, capillary water can be formed locally due to the
87 interaction force between water molecules (surface tension) (Weil and Brady, 2017a). The bound and capillary water states
88 can correspond to the equilibrium states of water and vapor inside unsaturated soil.

89 The system is in non-equilibrium when the water evaporation rate in the local region exceeds the vapor condensation rate. The
90 relative humidity is less than 100%, and the bound and capillary water is reduced while the vapor increases. The density of
91 vapor in the region gradually rises as the evaporation process proceeds, resulting in an increase in the probability of vapor
92 water molecules colliding with each other and the quantity of vapor water molecules absorbed by the water surface, which
93 indicates the vapor condensation rate accelerating. The system is in thermodynamic equilibrium when the evaporation and
94 condensation rates are equal, at which time the temperature and the concentration of water and vapor are constant, and the



95 relative humidity is 100%. In addition, the matrix suction of soil is mechanically balanced with the gravity of the bonded and
 96 capillary water. The system is in non-equilibrium when the condensation rate exceeds the evaporation rate. Vapor is
 97 supersaturated, the relative humidity is greater than 100%, and condensation occurs. The gravity of the bound and capillary
 98 water is greater than the matrix suction of the soil due to the generated condensate, resulting in gravity water of motion.



99
 100 1) Soil particles, 2) Bound water, 3) Pore, 4) Capillary water, 5) Gravity water, 6) Evaporation rate,
 101 7) Condensation rate, 8) Water surface

102 Fig. 1 The states and transformation of water in relation to equilibrium in unsaturated soils

103 **2.2 Water content calculation method**

104 **2.2.1 Calculating principle**

105 When the unsaturated soil is in thermodynamic equilibrium (100% relative humidity) at a certain temperature, the
 106 concentration of water and vapor is constant, as is the concentration ratio. When the external temperature changes, the
 107 equilibrium state of the system is destroyed, and water and vapor alter their relative content by evaporation or condensation to
 108 generate a new thermodynamic equilibrium state. At this time, the concentration and ratio of water and vapor are constant,
 109 although different from the value of the previous equilibrium state. Therefore, the concentration ratio of water to vapor at
 110 thermodynamic equilibrium is a function of temperature. We can establish the function experimentally, after which the soil
 111 water content can be determined by the function, provided that the soil temperature at thermodynamic equilibrium is obtained.

112 **2.2.2 Formula derivation**

113 Water in unsaturated soils exists in liquid and vapor forms at atmospheric temperature, and the masses of the two can be
 114 represented as

$$m_{water}(T) = \rho_{water}(T) \times V_{water}(T) \quad (1)$$



$$m_{vapor}(T) = \rho_{vapor}(T) \times V_{vapor}(T) \quad (2)$$

115 where $m_{water}(T)$ (kg), $\rho_{water}(T)$ (kg/m³), and $V_{water}(T)$ (m³) represent the mass, density, and volume of water at a temperature of
116 T (°C), respectively; $m_{vapor}(T)$ (kg), $\rho_{vapor}(T)$ (kg/m³), and $V_{vapor}(T)$ (m³) represent the mass, density, and volume of vapor at the
117 temperature of T (°C), respectively.

118 The composition and its concentration are constant when water and vapor in unsaturated soils are in thermodynamic
119 equilibrium, as shown in Eq. (3).

$$\frac{m_{water}(T)}{m_{vapor}(T)} = \frac{\rho_{water}(T) \times V_{water}(T)}{\rho_{vapor}(T) \times V_{vapor}(T)} = K(T) \quad (3)$$

120 where $K(T)$ is the thermodynamic equilibrium constant of the system at the temperature of T (°C), and its value is temperature-
121 dependent.

122 Assume that $\alpha(T)$ and $\beta(T)$ are the mass and density ratios of water to vapor, respectively, as follows

$$\frac{m_{water}(T)}{m_{vapor}(T)} = \alpha(T) \quad (4)$$

$$\frac{\rho_{water}(T)}{\rho_{vapor}(T)} = \beta(T) \quad (5)$$

123 The pores of the unsaturated soils are filled with air and water. According to Dalton's law of partial pressure, the volume of
124 air equals that of vapor. Hence the relationship between the volume of pores, water, and vapor is shown in Eq. (6) (Hillel,
125 2008b).

$$V_p = V_{water} + V_{vapor} \quad (6)$$

126 where V_p (m³) denotes the volume of pores in unsaturated soils; V_{water} (m³) denotes the volume of water; and V_{vapor} (m³) denotes
127 the volume of vapor.

128 Equation (7) is obtained by combining Eq. (3), Eq. (4), Eq. (5), and Eq. (6),

$$\alpha(T) = \beta(T) \times \frac{V_{water}(T)}{V_p - V_{water}(T)} \quad (7)$$

129 Therefore, the volumetric water content in the unsaturated soils is

$$W_V(T) = \frac{V_{water}(T)}{V_s} \times 100\% = \frac{\alpha(T) \times V_p}{\alpha(T) + \beta(T)} \times 100\% \quad (8)$$

130 where $W_V(T)$ (%) represents the volumetric water content in unsaturated soils; V_s (m³) represents the unit volume of soils.

131 As a result, determining the mass and density ratio of water to vapor is fundamental for calculating soil's volumetric water
132 content.



133 2.3 The density of water and vapor and their ratio

134 Research data on the properties of saturated water and vapor at different temperatures have been published by the International
 135 Association for the Properties of Water and Steam (IAPWS) (The International Association for the Properties of Water and
 136 Steam, 2007), Wagner, Kruse (1998), and Kretzschmar et al. (2019), which obtained using equations for the thermophysical
 137 properties of water and steam. The density and density ratio of water and vapor are analysed in this study using the above data.
 138 Although water is the most common liquid in nature, it is also the most unusual, with many peculiar properties, the most
 139 obvious of which is the anomalous density, which is closely related to its complicated molecular structure and configuration
 140 (Gallo et al., 2016; Pettersson et al., 2016). As water molecules are polar, they may be joined by hydrogen bonds to form a
 141 more stable tetrahedral structure, and many water molecules and hydrogen bonds can construct a complex and huge network
 142 (Hillel, 1971; Sciortino and Fornili, 1989).

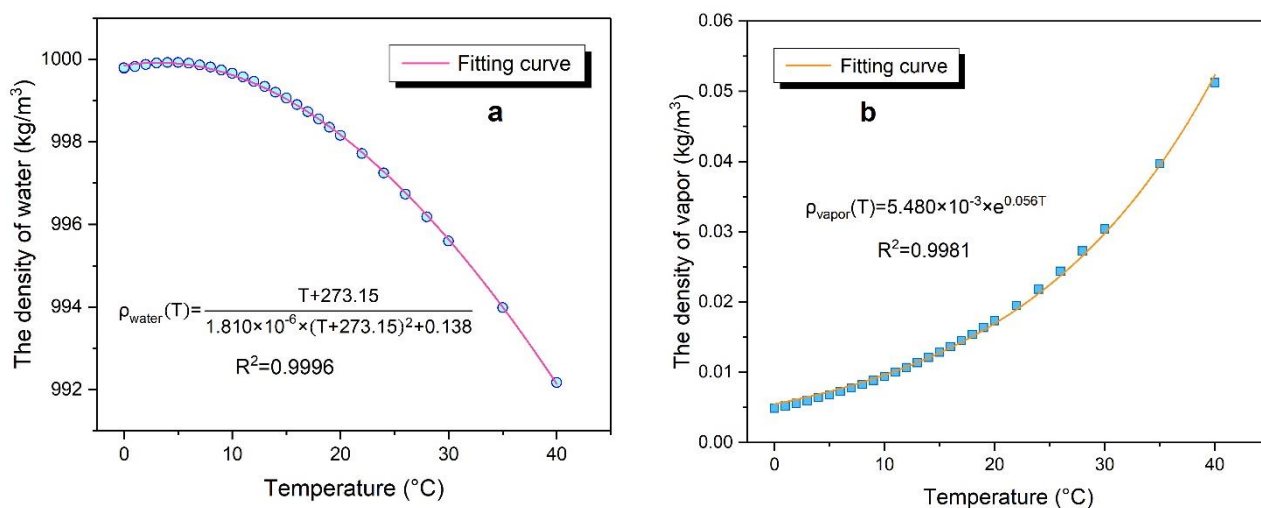


Fig. 2 The density varies with temperature a) water; b) vapor

143 The structure of water molecules is complicated in the range of 0-4°C, with the coexistence of free molecules, chains, clusters,
 144 hexagonal structures, and ice crystals. In addition, the tetrahedron structure of hydrogen-bonded network of molecules with
 145 larger volume in ice are partially destructed with increasing temperature, which results in water molecules falling into the
 146 cavity of residual tetrahedron (Pang, 2014). Thus, the free volume of water reduces while the density increases and reaches a
 147 maximum at 4°C (Mahoney and Jorgensen, 2000; Poole et al., 1992). Then, as the temperature continues to rise, the hydrogen
 148 bonding network structure is destroyed, and the distance between water molecules increases, resulting in an increase in water
 149 volume and a decrease in density. According to the study of Yue (1992), the relationship between water density and
 150 temperature is as follows.

$$\rho_{water}(T) = \frac{T + 273.15}{1.810 \times 10^{-6} \times (T + 273.15)^2 + 0.138} \quad R^2=0.9996 \quad (9)$$

151 The greater the temperature, the more intense the thermal movement of water molecules, resulting in more water vapor
 152 molecules to overcome intermolecular forces (such as electrostatic forces, induction forces, dispersion forces, etc.) (Eisenberg



153 and Kauzmann, 2007), increasing the number of vapor molecules in the air and the density of vapor. Furthermore, vapor
154 density varies exponentially with temperature, and the fitting equation is as follows.

$$\rho_{vapor}(T) = 5.480 \times 10^{-3} \times e^{0.056T} \quad R^2=0.9981 \quad (10)$$

155 Figure 3 shows the variation of density ratio of water to vapor with temperature. Water density fluctuates slightly at
156 atmospheric temperature, decreasing only from 0.99992 g/cm³ at 4°C to 0.99922 g/cm³ at 40 °C, whereas vapor density varies
157 exponentially with temperature. Therefore, the density ratio of water to vapor also varies exponentially with temperature, and
158 the fitting function is

$$\beta(T) = 2.037 \times 10^5 \times e^{-0.064T} \quad R^2=0.9991 \quad (11)$$

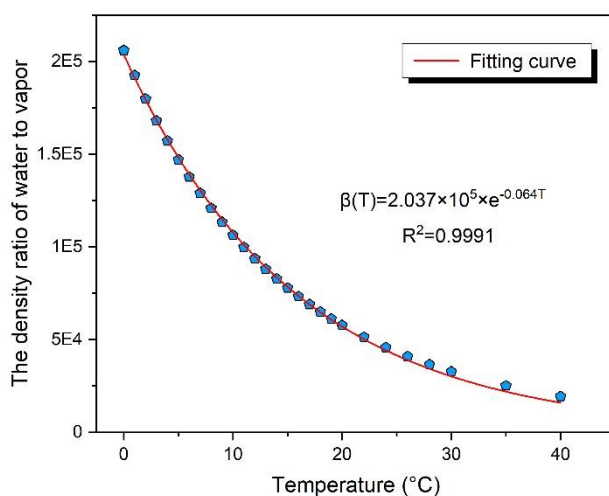


Fig. 3 The density ratio of water to vapor varies with temperature

159
160
161
162
163
164
165
166
167
168



169 **3 Material and methods**

170 **3.1 Soil samples**

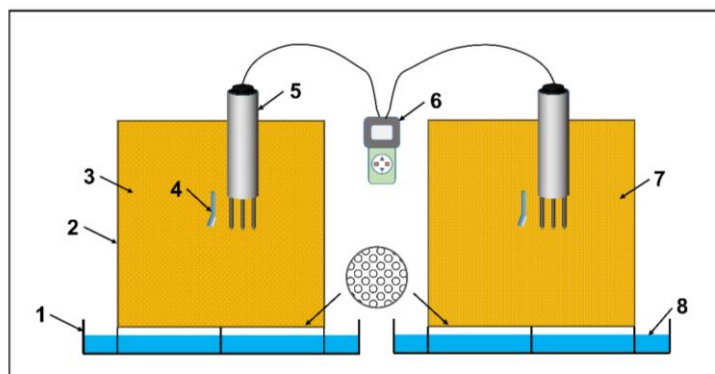
171 The soil samples in this study were collected in Jinan, Shandong Province, China. The soil samples were air-dried, ground,
172 and passed through 30 mesh, 60 mesh, and 200 mesh sieves in turn to produce medium and fine sand, which were then filled
173 into the sandboxes. Soil samples were taken with cutting rings at 5 cm, 15 cm, and 25 cm depths in two sandboxes at the end
174 of the experiment, and the water content, natural density, and dry density were determined by weighing the soil samples before
175 and after drying in an oven at 105 °C for 48 hours (Topp et al., 2007). The gravimetric method with water saturation was used
176 to determine the porosity of soil samples (Flint and Flint, 2002). The properties of medium and fine sand are shown in Table
177 1.

178 Table 1 Properties of the two tested soils

Soil textures	Particle size (mm)	Natural density (g/cm ³)	Dry density (g/cm ³)	Porosity (%)
Medium sand	0.075 - 0.25	1.72	1.43	35.44
Fine sand	0.25 – 0.50	1.99	1.63	45.75

179 **3.2 Experimental setup**

180 To obtain the content of water and vapor at different temperatures at thermodynamic equilibrium in soils, we conducted
181 observing experiments. The experimental apparatus comprises three parts: a water vapor replenishment device, a measurement
182 device, and a data collection device, as shown in Fig. 4. The water vapor replenishment device is a 40 cm × 40 cm × 5 cm top
183 open tank. The measurement device consists of sandboxes and sensors. The dimensions of the sandboxes are 30 cm × 30 cm
184 × 30 cm, and there are 5mm diameter holes distributed in the bottom in the shape of quincunx to allow water vapor from the
185 tank to enter the sandboxes. When filling the sandboxes, the soil is compacted using the water-saturated exhaust method to
186 ensure homogeneity. The temperature and humidity sensors (iButton DS1923, Maxim, USA) measured and recorded the
187 temperature and relative humidity inside the sandboxes. The temperature measurement range is -20-85 °C, with a ± 0.10 °C
188 precision; the relative humidity measurement range is 0-120%, with a ± 0.04% accuracy. The volumetric water content in
189 sandboxes is measured by a soil water content sensor (SYC-SFQ, Saiyasi Technology, China) in the range of 0-100% with ±
190 2% accuracy. The data collection device (SYD-1, Saiyasi Technology, China) was used to collect and store soil water content.
191 The tanks and sandboxes are made of 5 mm thick polymethyl methacrylate (PMMA).



1) Tank, 2) Sandbox, 3) Medium sand, 4) Temperature and humidity sensor, 5) Soil water sensor,
6) Data collector, 7) Fine sand, 8) Water

Fig. 4 Experimental apparatus

192
193
194
195

196 3.3 Data collection and processing

197 The experiment was conducted on the roof of the School of Environmental Studies, China University of Geosciences (Wuhan)
198 in a completely open natural environment. Changes in external circumstances produce variations in soil temperature and water
199 content. The experiment began in June 2020 and ended in January 2021. Temperature, humidity, and soil water content were
200 all measured at a rate of one time per minute. More than 100,000 data sets were collected during the experimental period.
201 Nonetheless, the majority of the data sets were collected while the system was in a non-equilibrium state, necessitating data
202 filtering. The data sets at 100% relative humidity were retained for further analysis and calculation.

203 The collected temperature values were brought into Eq. (9) and Eq. (10) respectively to get the density of water and vapor at
204 that temperature. The volume of water per unit volume of soil is the collected soil water content, and the volume of vapor can
205 be calculated using Eq. (6). The masses of water and vapor at this temperature can be determined according to Eq. (1) and Eq.
206 (2), and their mass ratios can be calculated using Eq. (4).

207 3.4 Significance test

208 Fisher's Permutation test was performed on the data sets to examine whether there was a significant difference in the mass
209 ratio functions of water to vapor in different media. The principle is to compare whether there is a difference between the
210 coefficients of the fitting functions of the two data sets. The mass ratio functions of water to vapor in medium and fine sand
211 are as follows, respectively.

$$\alpha_1(T) = a_1 e^{b_1 T} \quad (12)$$

$$\alpha_2(T) = a_2 e^{b_2 T} \quad (13)$$



212 The coefficient differences between the two models are defined as $c = a_1 - a_2$ and $d = b_1 - b_2$, and the null hypothesis of
213 the test is $H_0: c = 0, d = 0$.

214 The models (12) and (13) were fitted to the data of the medium and fine sand groups, respectively, and the initial estimates of
215 the coefficients $\hat{a}_1, \hat{a}_2, \hat{b}_1$ and \hat{b}_2 , and the coefficients difference ($\hat{c}_0 = \hat{a}_1 - \hat{a}_2$ and $\hat{d}_0 = \hat{b}_1 - \hat{b}_2$) between the two groups
216 were obtained.

217 The medium sand data sets (n_1 data sets) and the fine sand data sets (n_2 data sets) were combined to produce a sample S
218 consisting of $n_1 + n_2$ observations. From the sample S , n_1 observations were randomly selected (without replacement) and
219 considered as the "medium sand data sets" (denoted as S_m), while the remaining n_2 observations were considered as the "fine
220 sand data sets" (denoted as S_f). For empirical samples S_m and S_f , models (12) and (13) were fitted to obtain $\hat{a}_1^{S_1}, \hat{a}_2^{S_1}, \hat{b}_1^{S_1}$ and
221 $\hat{b}_2^{S_1}$ (S_1 denotes the first sampling), as well as the coefficients difference ($c^{S_1} = \hat{a}_1^{S_1} - \hat{a}_2^{S_1}$ and $d^{S_1} = \hat{b}_1^{S_1} - \hat{b}_2^{S_1}$) between the
222 two groups.

223 Repeating the process of sampling and calculating the coefficient differences 1000 times, the empirical distribution of
224 coefficients difference c^{S_j}, d^{S_j} ($j=1, 2, \dots, 1000$) can be determined.

225 Therefore, the empirical p-value can be expressed as

$$\hat{p}_c = \frac{\#\{c^{S_j} > \hat{c}_0\}}{1000} \quad (14)$$

$$\hat{p}_d = \frac{\#\{d^{S_j} > \hat{d}_0\}}{1000} \quad (15)$$

226 where $\#\{c^{S_j} > \hat{c}_0\}$ and $\#\{d^{S_j} > \hat{d}_0\}$ denote the number of c^{S_j} and d^{S_j} that are greater than the initial estimates \hat{c}_0 and \hat{d}_0 ,
227 respectively.

228 The null hypothesis can be rejected at the 5% level if the empirical p-value is less than 0.05, indicating that the coefficients
229 difference between the two groups of data is significant; otherwise, the coefficients difference is not significantly different at
230 the 5% level.

231 All of the above processes were performed in Stata 16.

232 4 Results and Discussions

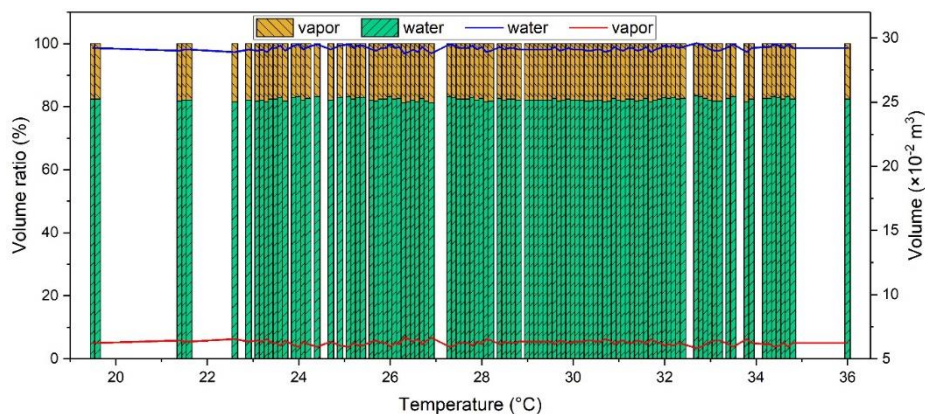
233 4.1 The volume of water and vapor

234 Figure 5 and Figure 6 depict the fluctuation in volume and volume proportion of water and vapor within medium and fine sand
235 at different equilibrium temperatures (The volume of water and vapor is the content of 1m^3 of soil). Since the porosity of
236 medium sand is lower than that of fine sand, the volume of water and vapor in medium sand is less.

237 The volumes of water and vapor fluctuate with temperature in both medium and fine sand, while the overall change is small,
238 and the variation is more significant in medium sand than that in fine sand. The volumetric water content of the soil is affected

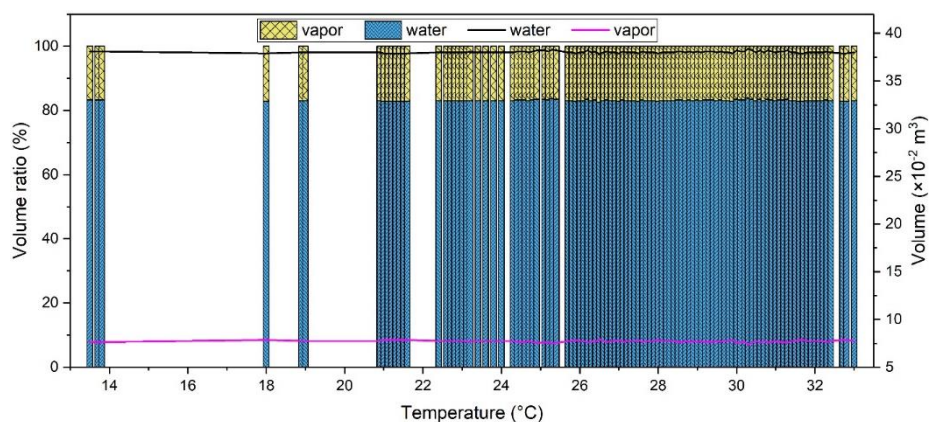


239 by temperature, according to Kocarek and Kodesova (2012). We consider that temperature has two effects on volumetric water
240 content: on the one hand, temperature changes affect the density of water and vapor, resulting in variations in their volume; on
241 the other hand, it may alter the equilibrium of water and vapor, leading to changes in their relative contents. In this study, the
242 density of water fluctuates less at atmospheric temperature, and thus its volume changes slightly. Furthermore, due to the
243 limitations of sensors' precision, the volume changes of water and vapor while they are in equilibrium are challenging to
244 determine accurately. Therefore, the correlation between temperature and volume of water and vapor is weak.



245
246

Fig. 5 Variation of the volume of water and vapor with temperature in medium sand



247
248

Fig. 6 Variation of the volume of water and vapor with temperature in fine sand

249 Although there are differences in the volume of water and vapor between medium and fine sand, the volume ratio of the two
250 is almost consistent, about 83%:17%. As a result, the volume ratio of water to vapor in soils is less dependent on soil properties
251 at thermodynamic equilibrium.



252 4.2 The mass ratio of water and vapor

253 4.2.1 The mass ratio in different media

254 The concentration of water and vapor and their mass ratio in unsaturated soil is constant when the system is in thermodynamic
 255 equilibrium. Moreover, temperature variations impact the equilibrium state of water and vapor, leading to changes in their
 256 relative contents. Thus, this section will discuss the mass ratio of water to vapor as a function of temperature. The masses of
 257 water and vapor and their mass ratio are calculated by Eq. (1), Eq. (2), and Eq. (4), respectively. This study obtained 254 sets
 258 of equilibrium state data in medium sand and 231 in fine sand. 90% of the data sets are utilized for the analysis of the mass
 259 ratio of water to vapor in relation to temperature, and the remaining data sets are used for the reliability analysis in section 4.3.
 260 The variation of the mass ratio of water to vapor in medium and fine sand with temperature is depicted in Fig. 7a and Fig. 7b,
 261 respectively. The equilibrium points in medium and fine sand are primarily dispersed in the 22-34 °C temperature range. When
 262 the temperature is low, the intensity of water evaporation is weak, and the water conversion rate into vapor is slow, resulting
 263 in low vapor content in the pore and a non-equilibrium condition. The water conversion rate to vapor increases as the
 264 temperature rises, resulting in an increase in the water vapor content and the probability of an equilibrium condition.

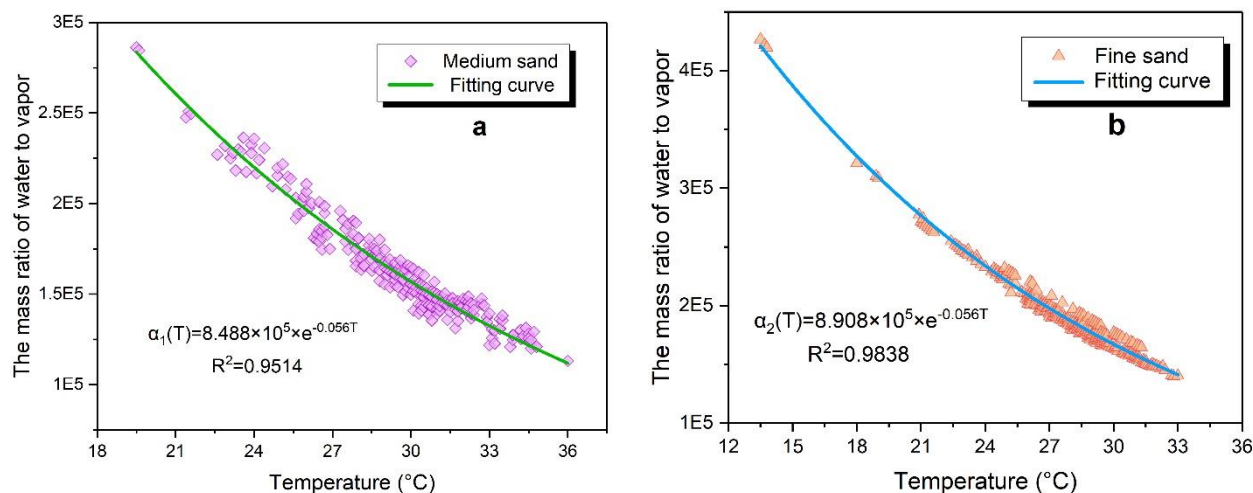


Fig. 7 The mass ratios of water to vapor vary with temperature a) medium sand; b) fine sand

265 The mass ratios of water to vapor decrease exponentially with increasing temperature. The density of water decreases slightly
 266 as the temperature rises (experiment temperatures are above 4 °C). In contrast, the vapor density increases exponentially, and
 267 the volume ratios of water to vapor in medium and fine sand are almost constant, according to section 4.1. As a result, the
 268 mass ratios of water to vapor vary with temperature similarly to their density ratios, and both decrease exponentially. The
 269 fitting equations for the mass ratio of water to vapor and temperature in medium and fine sand, respectively, are

$$\alpha_1(T) = 8.488 \times 10^5 \times e^{-0.056T} \quad R^2=0.9515 \quad (16)$$

$$\alpha_2(T) = 8.908 \times 10^5 \times e^{-0.056T} \quad R^2=0.9838 \quad (17)$$



270 **4.2.2 Significance of difference analysis**

271 The difference in specific surface area between the medium and fine sand used in this study is due to a variation in particle
 272 size, which resulted in different adsorption forces on water and vapor and moisture content discrepancies (Khlosi et al., 2013).
 273 According to the analysis in sections 2.1 and 2.2, when the unsaturated soil is in thermodynamic equilibrium, the system is in
 274 mechanical equilibrium, and the mass ratio of water to vapor is constant, at which the adsorption forces are balanced with the
 275 gravity of water. Consequently, the mass ratio of water to vapor is the same in medium sand, fine sand, or other media at the
 276 same temperature in thermodynamic equilibrium. While the form of the equations for the mass ratios of water to vapor in
 277 medium and fine sand determined in this study is consistent, there are differences in the specific coefficients. In this section,
 278 we utilize Fisher's Permutation test to examine whether the mass ratio functions of water to vapor in different mediums differ
 279 significantly.

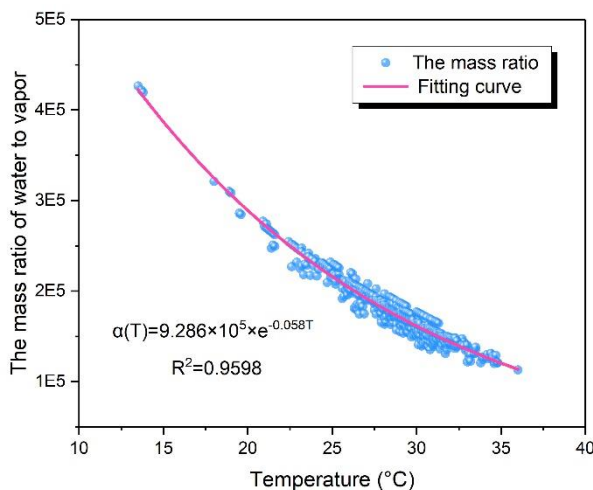
280 Table 2 shows the results of Fisher's Permutation test on the data of the mass ratios of water to vapor in medium and fine sand.

281 Table 2 Results of the one-way analysis of variance

Variables	The initial coefficients		The coefficients difference	Frequency	Empirical <i>p</i> -value
	Medium sand	Fine sand			
a	8.488×10^5	8.908×10^5	-4.199×10^4	942	0.942
b	-0.0563	-0.0558	-5.577×10^{-4}	728	0.728

282 There is no significant difference between the mass ratio and the water-containing media because the empirical *p*-value is
 283 larger than 0.05, indicating that the mass ratio has no connection with the nature of the medium. Therefore, the final mass ratio
 284 could be obtained by fitting all of the data on the mass ratio of water to vapor at thermodynamic equilibrium in medium and
 285 fine sand (Fig. 8). The fitting equation is as follows.

$$\alpha(T) = 9.286 \times 10^5 \times e^{-0.058T} \quad R^2=0.9598 \quad (18)$$



286

287

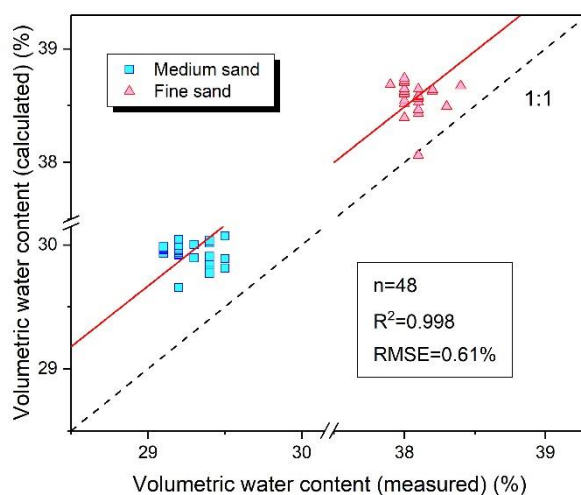
Fig. 8 The mass ratio of water to vapor varies with temperature



288 **4.3 Reliability analysis**

289 Sections 2.3 and 4.2 determine the density ratio and mass ratio of water to vapor, respectively, so the water content of
 290 unsaturated soil could be calculated using Eq. (8). The remaining equilibrium data sets (i.e., 25 sets of medium sand and 23
 291 sets of fine sand) are utilized for reliability analysis in this section to evaluate the accuracy of the method. The density ratio
 292 and mass ratio are calculated using the temperatures in the data sets, and then they are substituted into Eq. (8) to determine the
 293 soil volumetric water content, which was then compared to the measured values.

294 Figure 9 shows the calculated volumetric water content compared to the actual measured. Table 3 shows the statistical results
 295 of the absolute errors in the calculated volumetric water content. According to Fig. 9 and Table 3, the absolute errors of the
 296 calculated volumetric water content is minimal. The means of the absolute error of the volumetric water content in medium
 297 and fine sand are 0.66% and 0.49%, and the maximums are 0.88% and 0.78%, respectively, indicating the method is accurate
 298 and reliable. The root mean square error (RMSE) of all data points is 0.61%, and the data points are basically above the 1:1
 299 line, which indicates that the volumetric water content calculated is slightly greater than the measured. Moreover, there are
 300 two reasons for the absolute error: the first is the deviation in position of the temperature, humidity, and volumetric water
 301 content sensors during the experiment; the second is the error of the experimental apparatus, particularly the volumetric water
 302 content sensor, which has a 2% error.



303
 304
 305

Fig. 9 Comparison of the volumetric water content measured and calculated

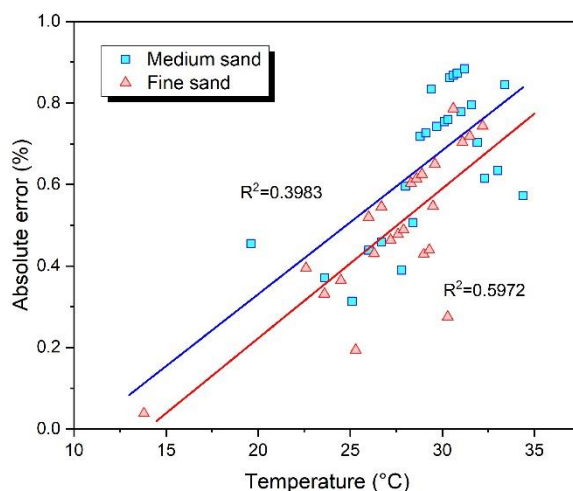
Table 3 The statistical results of absolute error of volumetric water content

Soil textures	Mean/%	Standard deviation/%	Maximum/%	Maximum/%
medium sand	0.66	0.18	0.88	0.31
fine sand	0.49	0.18	0.79	0.04

306 Furthermore, the standard deviation of absolute error of volumetric water content is 0.18% in both medium and fine sand,
 307 indicating a significant degree of dispersion. Then we proceed to analyse the absolute error as a function of temperature. The



308 absolute error is temperature dependent, as shown in Fig. 10, and tends to increase as the temperature rises. This is because
309 although the soil volumetric water content fluctuates with temperature, it has no significant correlation. In contrast, the
310 volumetric water content obtained by this study's method is positively correlated with temperature, resulting in a more
311 significant absolute error at higher temperatures.



312

313

Fig. 10 The absolute error of the volumetric water content varies with temperature

314 4.4 Potential application of the method

315 The time domain and frequency domain reflection methods are widely used for field soil water content measurement with an
316 absolute error higher than 2% (Jacobsen and Schjønning, 1993; Lekshmi et al., 2014). The method proposed in this study has
317 an absolute error of less than 1%, which is advantageous in terms of accuracy.

318 The method we proposed is applicable to the field as well as the laboratory. The volumetric water content can be determined
319 with Eq. (8) using the mass ratio by Eq. (18) and the density ratio by Eq. (11), using the measurements of soil porosity (or rock
320 fissure rate), temperature, and relative humidity. The relative humidity is not used in the estimation of the volumetric water
321 content but to determine whether the geotechnical system is in thermodynamic equilibrium. Only systems that are in
322 equilibrium or near equilibrium can use this method to estimate the water content.

323 To verify the applicability of the method, we conducted field experiments. We selected a woodland in Wuhan and placed
324 temperature and humidity monitors at different depths of the soil (0 cm, 10 cm, 20 cm, 40 cm, 80 cm, 100 cm), collecting
325 temperature and humidity data every 5 minutes. We found that the relative humidity in the soil under natural conditions in the
326 field was mostly concentrated at 99%-101% after one week of continuous measurement, which indicates that the water and
327 vapor in the soil are in near equilibrium under natural conditions, so the soil water content can be determined directly using
328 the method we proposed. The results are shown in Table 4.

329

330



331

Table 4 The measurement results of soil at different depths

	0 cm	10 cm	20 cm	40 cm	80 cm	100 cm
Temperature/°C	19.37	19.45	19.98	20.47	21.65	21.79
Relative humidity/%	100.9	99.6	97.0	98.5	100.4	100.4
Water content/%	27.78	27.78	27.79	27.81	27.84	27.84

332 The great potential application for this method is determining the water content of rocks. Water content measurements in soil
333 are fairly mature, whereas it is still more complicated in rocks due to sampling difficulties and near-closed fissures. The above
334 studies have confirmed that the density and mass ratios of water to vapor are independent of the nature of the water-containing
335 medium, therefore the method is applicable to any medium. We drilled a hole that has a diameter of 10 cm, a depth of 200 cm
336 in the rock wall of an abandoned quarry in Jinan, Shandong Province. Temperature and humidity monitors were also placed
337 at different depths (0 cm, 10 cm, 20 cm, 40 cm, 60 cm, 100 cm, and 150 cm) to collect temperature and humidity data in the
338 rock. The results showed that the relative humidity in the rock was also concentrated at 99%-101%, so the method can be
339 directly applied to calculate the water content in the rocks. The water content within each depth of the rock was calculated to
340 be approximately 0.612%, and the result would be validated subsequently.

341

Table 5 The measurement results of rock at different depths

	0 cm	10 cm	20 cm	40 cm	60 cm	100 cm	150 cm
Temperature/°C	16.70	17.93	17.85	17.90	18.00	18.65	19.53
Relative humidity/%	43.8	99.3	100.6	100.9	100.6	100.2	100.1
Water content/%	/	0.612	0.612	0.612	0.612	0.612	0.613

342 According to our monitoring and investigation in North and Central China, soils and rocks up to a depth of 100 cm and 150
343 cm, respectively, are in equilibrium or near equilibrium under natural conditions, so the volumetric water content of soils and
344 rocks can be estimated using this method. Nevertheless, the application of the method will be restricted in some areas with dry
345 climates (such as northwest China and the western United States), where the water content in rock-soil mass and air is low and
346 the system is non-equilibrium the vast majority of the time. In this situation, it is necessary to choose the appropriate time for
347 measuring the water content of the rock-soil mass. A temporary equilibration of the system occurs between dusk and dawn,
348 when the ambient temperature decreases, resulting in a condensation process in rock-soil mass. It is the proper time to
349 determine water content.

350 5 Conclusions

351 In this study, we proposed an alternative method to measure soil water content using the ratios of mass and density of water to
352 vapor based on system science and thermodynamics. We derived the mass ratio and density ratio of water to vapor as a function
353 of temperature from published data and validated the accuracy of the proposed method using observed temperature, relative



354 humidity, and volumetric water content in two soil textures of medium and fine sand. We further demonstrated that the mass
355 ratio function is independent of the nature of the water-containing media using theoretical and statistical analysis. The absolute
356 error of soil water content between the calculated and measured ones is less than 1% and is positively correlated with
357 temperature. When the geotechnical system is in equilibrium or near equilibrium, the water content can be calculated by the
358 method we proposed. According to monitoring and investigation, soils and rocks up to a depth of 100 cm and 150 cm,
359 respectively, are in equilibrium or near equilibrium under natural conditions, so the volumetric water content of rock-soil mass
360 can be estimated using this method. This study significantly improves the measurement accuracy of soil water content,
361 eliminates the effect of water-containing medium on soil water content measuring, and has excellent potential for application
362 in the field soil and even rock water content measurement.

363 **Data availability**

364 The data that support the findings of this study are available from the corresponding author upon reasonable request.

365 **Author contribution**

366 **Danhui Su:** Conceptualization, Data curation, Writing - original draft. **Jianwei Zhou:** Methodology, Conceptualization,
367 Writing – review & editing. **Zuocong Yin:** Methodology, Investigation, Formal analysis. **Haibo Feng:** Methodology,
368 Investigation, Writing – review & editing. **Xiaoming Zheng:** Investigation, Validation. **Xu Han:** Investigation. **Qingqiu Hou:**
369 Investigation.

370 **Competing interests**

371 All co-authors have seen and agree with the contents of the manuscript. We declare that we have no known competing financial
372 interests or personal relationships that could have appeared to influence the work reported in this paper.

373 **Acknowledgments**

374 The authors gratefully acknowledge financial support from the National Natural Science Foundation of China (No. 42077182).
375 We are also extremely grateful to Prof. Hengli Xu for assistance on the experimental design.

376 **References**

377 Alessi, R.S., Prunty, L., 1986. Soil-water determination using fiber optics. Soil Science Society of America Journal, 50(4):
378 860-863. DOI:<https://doi.org/10.2136/sssaj1986.03615995005000040006x>



- 379 Anh, N.V., Fukuda, S., Hiramatsu, K., Harada, M., 2015. Sensitivity-based calibration of the soil and water assessment tool
380 for hydrologic cycle simulation in the Cong Watershed, Vietnam. *Water Environment Research*, 87(8): 735-750.
381 DOI:<https://doi.org/10.2175/106143015X14338845156948>
- 382 Ansermet, J.P., Brechet, S.D., 2019. *Thermodynamics of subsystems, Principles of thermodynamics*. Cambridge University
383 Press, Cambridge, UK, pp. 49-69. DOI:<https://doi.org/10.1017/9781108620932.004>
- 384 Bogena, H.R. et al., 2015. Emerging methods for noninvasive sensing of soil moisture dynamics from field to catchment scale:
385 A review. *Wiley Interdisciplinary Reviews: Water*, 2(6): 635-647. DOI:<https://doi.org/10.1002/wat2.1097>
- 386 Braudeau, E., Mohtar, R.H., 2021. Hydrostructural pedology, culmination of the systemic approach of the natural environment.
387 *Systems*, 9(1): 8. DOI:<https://doi.org/10.3390/systems9010008>
- 388 Breda, N., Huc, R., Granier, A., Dreyer, E., 2006. Temperate forest trees and stands under severe drought: A review of
389 ecophysiological responses, adaptation processes and long-term consequences. *Annals of Forest Science*, 63(6): 625-644.
390 DOI:<https://doi.org/10.1051/forest:2006042>
- 391 Brockett, B.F.T., Prescott, C.E., Grayston, S.J., 2012. Soil moisture is the major factor influencing microbial community
392 structure and enzyme activities across seven biogeoclimatic zones in western Canada. *Soil Biology and Biochemistry*, 44(1):
393 9-20. DOI:<https://doi.org/10.1016/j.soilbio.2011.09.003>
- 394 Cui, H.N., 2009. *Phase transitions in unary system, Thermodynamic system theory*. Jilin University Press, Changchun, China,
395 pp. 56-76.
- 396 Daly, E., Porporato, A., 2005. A review of soil moisture dynamics: From rainfall infiltration to ecosystem response.
397 *Environmental Engineering Science*, 22(1): 9-24. DOI:<https://doi.org/10.1089/ees.2005.22.9>
- 398 Dexter, A.R., Czyż, E.A., Richard, G., 2012. Equilibrium, non-equilibrium and residual water: Consequences for soil water
399 retention. *Geoderma*, 177-178: 63-71. DOI:<https://doi.org/10.1016/j.geoderma.2012.01.029>
- 400 Eisenberg, D., Kauzmann, W., 2007. *The real vapour, The structure and properties of water*. Oxford University Press, New
401 York, US, pp. 36-70. DOI:<https://doi.org/10.1093/acprof:oso/9780198570264.003.0002>
- 402 Flint, L.E., Flint, A.L., 2002. 2.3 Porosity. In: Dane, J.H., Topp, G.C. (Eds.), *Methods of soil analysis, Part 4-Physical methods*.
403 Soil Science Society of America, Madison, US, pp. 241-254. DOI:<https://doi.org/10.2136/sssabookser5.4.c11>
- 404 Gallo, P. et al., 2016. Water: A tale of two liquids. *Chemical Reviews*, 116(13): 7463-7500.
405 DOI:<https://doi.org/10.1021/acs.chemrev.5b00750>
- 406 Good, S.P., Noone, D., Bowen, G., 2015. Hydrologic connectivity constrains partitioning of global terrestrial water fluxes.
407 *Science*, 349(6244): 175-177. DOI:<https://doi.org/10.1126/science.aaa5931>
- 408 Hillel, D., 1971. Physical properties of water. In: Hillel, D. (Ed.), *Soil and water: Physical principles and processes*. Academic
409 Press, New York, US, pp. 29-48. DOI:<https://doi.org/10.1016/B978-0-12-348550-2.50008-X>
- 410 Hillel, D., 1980. Soil water: Content and potential. In: Hillel, D. (Ed.), *Fundamentals of Soil Physics*. Academic Press, San
411 Diego, pp. 123-165. DOI:<https://doi.org/10.1016/B978-0-08-091870-9.50012-1>



- 412 Hillel, D., 2008a. Soil-water statics. In: Hillel, D. (Ed.), Soil in the environment. Academic Press, San Diego, US, pp. 79-89.
413 DOI:<https://doi.org/10.1016/B978-0-12-348536-6.50011-3>
- 414 Hillel, D., 2008b. Soil physical attributes. In: Hillel, D. (Ed.), Soil in the environment. Academic Press, San Diego, US, pp.
415 55-77. DOI:<https://doi.org/10.1016/B978-0-12-348536-6.50010-1>
- 416 Huisman, J.A., Hubbard, S.S., Redman, J.D., Annan, A.P., 2003. Measuring soil water content with ground penetrating radar:
417 A review. *Vadose Zone Journal*, 2(4): 476-491. DOI:<https://doi.org/10.2113/2.4.476>
- 418 Jackson, T.J., 2002. Remote sensing of soil moisture: implications for groundwater recharge. *Hydrogeol J*, 10(1): 40-51.
419 DOI:<https://doi.org/10.1007/s10040-001-0168-2>
- 420 Jacobsen, O.H., Schjønning, P., 1993. Field evaluation of time domain reflectometry for soil water measurements. *J Hydrol*,
421 151(2): 159-172. DOI:[https://doi.org/10.1016/0022-1694\(93\)90234-Z](https://doi.org/10.1016/0022-1694(93)90234-Z)
- 422 Jarvis, N.J., Leeds-Harrison, P.B., 1987. Some problems associated with the use of the neutron probe in swelling/shrinkling
423 clay soils. *Journal of Soil Science*, 38(1): 149-156. DOI:<https://doi.org/10.1111/j.1365-2389.1987.tb02132.x>
- 424 Khlosi, M. et al., 2013. Exploration of the interaction between hydraulic and physicochemical properties of Syrian soils.
425 *Vadose Zone Journal*, 12(4): 1-11. DOI:<https://doi.org/10.2136/vzj2012.0209>
- 426 Klenke, J.M., Flint, A.L., 1991. Collimated neutron probe for soil water content measurements. *Soil Science Society of*
427 *America Journal*, 55(4): 916-923. DOI:<https://doi.org/10.2136/sssaj1991.03615995005500040003x>
- 428 Kocarek, M., Kodesova, R., 2012. Influence of temperature on soil water content measured by ECH2O-TE sensors.
429 *International Agrophysics*, 26(3): 259-269. DOI:<https://doi.org/10.2478/v10247-012-0038-2>
- 430 Kretzschmar, H.J., Wagner, W., 2019. Tables of the properties of water and steam, *International steam tables: Properties of*
431 *water and steam based on the industrial formulation IAPWS-IF97*. Springer, Berlin, Germany, pp. 173-344.
432 DOI:https://doi.org/10.1007/978-3-662-53219-5_5
- 433 Lekshmi, S.U.S., Singh, D.N., Baghini, M.S., 2014. A critical review of soil moisture measurement. *Measurement*, 54: 92-
434 105. DOI:<https://doi.org/10.1016/j.measurement.2014.04.007>
- 435 Lim, H.H., Cheon, E., Lee, D.H., Jeon, J.S., Lee, S.R., 2020. Classification of granite soils and prediction of soil water content
436 using hyperspectral visible and near-infrared imaging. *Sensors*, 20(6): 1611. DOI:<https://doi.org/10.3390/s20061611>
- 437 Liu, X.B. et al., 2019. Measurement of soil water content using ground-penetrating radar: a review of current methods.
438 *International Journal of Digital Earth*, 12(1): 95-118. DOI:<https://doi.org/10.1080/17538947.2017.1412520>
- 439 Lu, N., Zhang, C., 2019. Soil sorptive potential: Concept, theory, and verification. *Journal of Geotechnical and*
440 *Geoenvironmental Engineering*, 145(4): 04019006. DOI:[https://doi.org/10.1061/\(ASCE\)GT.1943-5606.0002025](https://doi.org/10.1061/(ASCE)GT.1943-5606.0002025)
- 441 Ma, Y.H., Fan, X.J., 2020. Detection and analysis of soil water content based on experimental reflectance spectrum data. *Asia-*
442 *Pacific Journal of Chemical Engineering*, 15: e2507. DOI:<https://doi.org/10.1002/apj.2507>
- 443 Ma, Y.Y., Qu, L.Q., Wang, W., Yang, X.S., Lei, T.W., 2016. Measuring soil water content through volume/mass replacement
444 using a constant volume container. *Geoderma*, 271: 42-49. DOI:<https://doi.org/10.1016/j.geoderma.2016.02.003>



- 445 Mahoney, M.W., Jorgensen, W.L., 2000. A five-site model for liquid water and the reproduction of the density anomaly by
446 rigid, nonpolarizable potential functions. *Journal of Chemical Physics*, 112(20): 8910-8922.
447 DOI:<https://doi.org/10.1063/1.481505>
- 448 Manalo, F.P., Kantzas, A., Langford, C.H., 2003. Soil wettability as determined from using low-field nuclear magnetic
449 resonance. *Environ Sci Technol*, 37(12): 2701-2706. DOI:<https://doi.org/10.1021/es0259685>
- 450 Moroizumi, T., Sasaki, Y., 2008. Estimating the nonaqueous-phase liquid content in saturated sandy soil using amplitude
451 domain reflectometry. *Soil Science Society of America Journal*, 72(6): 1520-1526.
452 DOI:<https://doi.org/10.2136/sssaj2006.0212>
- 453 Ng Charles, W.W., Pang, Y.W., 2000. Influence of stress state on soil-water characteristics and slope stability. *Journal of*
454 *Geotechnical and Geoenvironmental Engineering*, 126(2): 157-166. DOI:[https://doi.org/10.1061/\(ASCE\)1090-](https://doi.org/10.1061/(ASCE)1090-)
455 [0241\(2000\)126:2\(157\)](https://doi.org/10.1061/(ASCE)1090-0241(2000)126:2(157))
- 456 Ni, X.Y., Liao, S., Wu, F.Z., Groffman, P.M., 2022. Microbial biomass in forest soils under altered moisture conditions: A
457 review. *Soil Science Society of America Journal*, 86: 358-368. DOI:<https://doi.org/10.1002/saj2.20344>
- 458 Nielsen, D.C., Lagae, H.J., Anderson, R.L., 1995. Time-domain reflectometry measurements of surface soil water content.
459 *Soil Science Society of America Journal*, 59(1): 103-105. DOI:<https://doi.org/10.2136/sssaj1995.03615995005900010016x>
- 460 Njoku, E.G., Entekhabi, D., 1996. Passive microwave remote sensing of soil moisture. *J Hydrol*, 184(1-2): 101-129.
461 DOI:[https://doi.org/10.1016/0022-1694\(95\)02970-2](https://doi.org/10.1016/0022-1694(95)02970-2)
- 462 Noborio, K., 2001. Measurement of soil water content and electrical conductivity by time domain reflectometry: A review.
463 *Computers and Electronics in Agriculture*, 31(3): 213-237. DOI:[https://doi.org/10.1016/S0168-1699\(00\)00184-8](https://doi.org/10.1016/S0168-1699(00)00184-8)
- 464 Norton, A.J. et al., 2022. Hydrologic connectivity drives extremes and high variability in vegetation productivity across
465 Australian arid and semi-arid ecosystems. *Remote Sensing of Environment*, 272: 112937.
466 DOI:<https://doi.org/10.1016/j.rse.2022.112937>
- 467 Pang, X.F., 2014. Molecular structures of water and its features, *Water: Molecular structure and properties*. World Scientific,
468 5 Toh Tuck Link, Singapore, pp. 1-88. DOI:https://doi.org/10.1142/9789814440431_0001
- 469 Pansu, M., Gautheyrou, J., 2006. Water content and loss on ignition, *Handbook of soil analysis. Mineralogical, organic and*
470 *inorganic methods*. Springer, Berlin, Germany, pp. 3-13. DOI:https://doi.org/10.1007/978-3-540-31211-6_1
- 471 Pettersson, L.G.M., Henchman, R.H., Nilsson, A., 2016. Water-The most anomalous liquid. *Chemical Reviews*, 116(13):
472 7459-7462. DOI:<https://doi.org/10.1021/acs.chemrev.6b00363>
- 473 Poole, P.H., Sciortino, F., Essmann, U., Stanley, H.E., 1992. Phase behaviour of metastable water. *Nature*, 360(6402): 324-
474 328. DOI:<https://doi.org/10.1038/360324a0>
- 475 Rahimi, A., Rahardjo, H., Leong, E.C., 2010. Effect of hydraulic properties of soil on rainfall-induced slope failure. *Eng Geol*,
476 114(3-4): 135-143. DOI:<https://doi.org/10.1016/j.enggeo.2010.04.010>
- 477 Robinson, D.A. et al., 2008. Soil moisture measurement for ecological and hydrological watershed-scale observatories: A
478 review. *Vadose Zone Journal*, 7(1): 358-389. DOI:<https://doi.org/10.2136/vzj2007.0143>



- 479 Satoh, Y., Kakiuchi, H., 2021. Calibration method to address influences of temperature and electrical conductivity for a low-
480 cost soil water content sensor in the agricultural field. *Agricultural Water Management*, 255: 107015.
481 DOI:<https://doi.org/10.1016/j.agwat.2021.107015>
- 482 Sciortino, F., Fornili, S.L., 1989. Hydrogen-bond cooperativity in simulated water: Time-dependence analysis of pair
483 interactions. *Journal of Chemical Physics*, 90(5): 2786-2792. DOI:<https://doi.org/10.1063/1.455927>
- 484 Sheets, K.R., Hendrickx, J.M.H., 1995. Noninvasive soil water content measurement using electromagnetic induction. *Water*
485 *Resour Res*, 31(10): 2401-2409. DOI:<https://doi.org/10.1029/95WR01949>
- 486 Shukla, M.K., 2013. Water in the vadose zone, *Soil physics: An introduction*. CRC Press, Boca Raton, US, pp. 119-156.
487 DOI:<https://doi.org/10.1201/b14926-10>
- 488 Strati, V. et al., 2018. Modelling soil water content in a tomato field: Proximal Gamma ray spectroscopy and soil–crop system
489 models. *Agriculture*, 8(4): 60. DOI:<https://doi.org/10.3390/agriculture8040060>
- 490 The International Association for the Properties of Water and Steam, 2007. Revised release on the IAPWS industrial
491 formulation 1997 for the thermodynamic properties of water and steam. International Association for the Properties of Water
492 and Steam, Lucerne, Switzerland.
- 493 Topp, G.C., Ferré, P.A., 2002. 3.1 Water content. In: Dane, J.H., Topp, G.C. (Eds.), *Methods of soil analysis, Part 4-Physical*
494 *methods*. Soil Science Society of America, Madison, US, pp. 417-545. DOI:<https://doi.org/10.2136/sssabookser5.4.c19>
- 495 Topp, G.C., Parkin, G.W., Ferré, P.A., 2007. Soil water content. In: Carter, M.R., Gregorich, E.G. (Eds.), *Soil sampling and*
496 *methods of analysis*. CRC Press, Boca Raton, US, pp. 939-962. DOI:<https://doi.org/10.1201/9781420005271-82>
- 497 Wagner, W., Kruse, A., 1998. Saturation state (Temperature table), *Properties of water and steam*. Springer, Berlin, Germany,
498 pp. 103-120. DOI:https://doi.org/10.1007/978-3-662-03529-0_9
- 499 Wang, Y.J., Lu, S., Ren, T.S., Li, B.G., 2011. Bound water content of air-dry soils measured by thermal analysis. *Soil Science*
500 *Society of America Journal*, 75(2): 481-487. DOI:<https://doi.org/10.2136/sssaj2010.0065>
- 501 Weil, R.R., Brady, N.C., 2017a. *Soil water: Characteristics and behavior, The nature and properties of soils*. Pearson Education,
502 London, UK, pp. 206-250.
- 503 Weil, R.R., Brady, N.C., 2017b. *The soils around us, The nature and properties of soils*. Pearson Education, London, UK, pp.
504 19-50.
- 505 Whalley, W.R., Dean, T.J., Izzard, P., 1992. Evaluation of the capacitance technique as a method for dynamically measuring
506 soil water content. *Journal of Agricultural Engineering Research*, 52(2): 147-155. DOI:[https://doi.org/10.1016/0021-8634\(92\)80056-x](https://doi.org/10.1016/0021-8634(92)80056-x)
- 507 8634(92)80056-x
- 508 Whalley, W.R., Ober, E.S., Jenkins, M., 2013. Measurement of the matric potential of soil water in the rhizosphere. *Journal of*
509 *Experimental Botany*, 64(13): 3951-3963. DOI:<https://doi.org/10.1093/jxb/ert044>
- 510 Xu, J.H., Ma, X.Y., Logsdon, S.D., Horton, R., 2012. Short, multineedle frequency domain reflectometry sensor suitable for
511 measuring soil water content. *Soil Science Society of America Journal*, 76(6): 1929-1937.
512 DOI:<https://doi.org/10.2136/sssaj2011.0361>



- 513 Xu, J.S., Yang, X.L., 2018. Three-dimensional stability analysis of slope in unsaturated soils considering strength nonlinearity
514 under water drawdown. Eng Geol, 237: 102-115. DOI:<https://doi.org/10.1016/j.enggeo.2018.02.010>
- 515 Yue, S., 1992. The density of water changes with temperature. University Chemistry, 7(3): 53-53.
516 DOI:<http://www.dxhx.pku.edu.cn/EN/10.3866/PKU.DXHX19920320>